E-ISSN 2581 – 7957
P-ISSN 2277 – 3916

CVR Journal of Science and Technology, Volume 22, June 2022
DOI: 10.32377/cvrjst2210

# Maximizing Power Yield from Mismatched Environment in Grid-Connected PV System by Fuzzy Logic Control

M. Krishnaprasad[1] and Vijay Raviprabhakaran[2]
[1]PG Scholar, CVR College of Engineering/EEE Department, Hyderabad, India
Email: krishna703.kp@gmail.com
[2]Assoc. Professor, CVR College of Engineering/EEE Department, Hyderabad, India
Email: vijai.mtp@gmail.com

***Abstract:*** **Solar power generation is one of the suggested methods of generating renewable energy due to its vast availability. Various concerns of the grid-connected photovoltaic (PV) system occur due to fluctuation in voltage and low efficiency. A fuzzy logic-based Buck-Boost converter (FLBBC) is proposed in this paper to produce constant voltage and increase the efficiency, when the PV arrays are exposed to different irradiance. The proposed FLBBC is operated either in buck or boost mode based on the output voltage of the PV subarray. The maximum power point (MPP) trackers are employed in each subarray. This ensures that both the subarrays are operated at their respective MPPT. A fuzzy logic controller is used for generating the necessary sinusoidal duty ratios for the switches of FLBBC. The different magnitudes of power are extracted from the two subarrays and delivered to the grid. When two different magnitudes of power are supplied to the grid it is needed to maintain the grid current sinusoidal and in phase with the grid voltage. The proposed FLBBC has been validated by comprehensive simulation in MATLAB. Furthermore, FLBBC can be employed in solar farms to maximize power yield and increase efficiency.**

***Index Terms:*** **Grid connected photovoltaic system, Fuzzy logic based Buck Boost converter, Maximum power point tracker, Different irradiance, Fuzzy logic controller.**

## I. Introduction

A photovoltaic (PV) system's primary goal is to guarantee the optimal performance of individual PV modules in a PV array when the modules are subjected to mismatched atmospheric conditions caused by differences in insolation level and operating temperature. The PV array's power output is considerably reduced when there is a discrepancy in module operating conditions. The issues related to mismatched operating conditions (MOC) become considerable when the number of series linked modules in a PV array is large. The required magnitude of input dc voltage of the inverter of a grid linked transformerless system is achieved by employing several series linked modules. As a result, during MOC, the power output of a grid linked transformerless (GLT) PV system, such as single-phase grid linked transformerless (SPGLT) inverter-based systems derived from H-bridge [1] and neutral node clamp (NNC) inverter-based systems [2] is significantly affected.

Various techniques have been described in the literature to solve the problem of MOC in a PV system. An in-depth examination of such approaches has been given in [3]. The power extraction during MOC can be enhanced by choosing suitable interconnections between PV modules [4] or by utilizing fuzzy logic controller algorithms to track the maximum power point (MPP) of the PV array [5]. Although, for low-power SPGLT PV systems, these approaches are ineffective. Similarly, reconfiguring PV modules in a PV array by altering the electrical connection of PV modules [6] is not effective for the SPGLT PV system because of the significant increase in component count and increase in operational complexity. During MOC, to get the most power out of each PV module. It has been attempted to control each PV module in a PV array using either a power electronic equalization or a dc-to-dc converter [7]. Power electronic equalization schemes need a large component count, increasing the system's cost and complexity of the operation. The technique described in [8] employs a Generation Governor Circuit (GGC) to run each PV module at its MPP, the difference in power between each module being processed only by the GGC. To improve power yield during MOC, the scheme proposed in [9] uses shunt current compensation of each module as well as series voltage compensation of each PV string in a PV array. Dedicated dc to dc converters is incorporated with each PV module in the systems based on module integrated converters [10]. However, the efficiency of the above-mentioned schemes is low due to the huge number of converter stages involved, and the component count in these schemes is high, thus they suffer from the same constraints as the power electronic equalization-based system. Instead of guaranteeing MPP functioning of every module, [11] link a specific number of modules in series to form a string, which is then made to work under MPP. Even yet, the total component count and control complexity do not decrease significantly.

Simplifying the control setup and reducing the component count schemes [12] combine all PV modules into two subarrays, and then each of the subarrays is made to operate at its respective MPP. However, both methods' overall efficiency is reported below. Power extraction during MOC is enhanced by adding a buck and boost stage to the SPGLT PV inverter. Furthermore, the demand for series linked PV modules in a PV array has decreased because of the presence of the intermediate boost stage. The switches of the dc-to-dc converter stage and the inverter stage work at high frequency in the schemes given in [13], resulting in a significant

Received on 26-07-2021, Revised on 06-11-2021, Accepted on 25-02-2022.

CVR Journal of Science and Technology, Volume 22, June 2022
DOI: 10.32377/cvrjst2210

reduction in the size of the passive element count and therefore increasing the operational efficiency of these schemes. Optimization techniques were also applied to optimal PV placement [14-16]

In this paper, an effort has been made to partition the PV modules into two serially linked sub-arrays, with each sub-array being controlled by a fuzzy logic-based buck and boost-based inverter to ensure optimum power evacuation from the sub-arrays during MOC. In comparison to the systems suggested in [17], this technique of separating an input PV array into two sub-arrays decreases the number of series linked modules in a sub-array by almost half. The suggested inverter's topological structure and control technique ensure that the magnitude of leakage current associated with PV arrays stays within the permitted range. Furthermore, as compared to the methods given in [18], the voltage stress across the active devices is reduced by approximately half. As a result, a very high-frequency operation is possible without increasing switching loss. The size of the passive components is also reduced because of the high-frequency operation. As a result, the suggested scheme's operational efficiency is high.

## II. Incremental Conductance method VS Fuzzy Logic Control

In the method of incremental conductance, when the light intensity on the PV array fluctuates, the output voltage may smoothly follow the fluctuations, preventing the power output oscillation from repeating at a steady state. The voltage swings are minor. It can change the logic style to decrease oscillation. The voltage fluctuation is modest compared to the P & O technique, making the technology ideal for quickly changing environmental conditions. This method is more sophisticated and performing A/D conversion will take a long time, causing problems managing the processor and placing a significant demand on hardware, particularly the precision of the sensor. Adjusting the step and threshold in the incremental conductance technique might be tricky. The tracking speed is determined by the size of the step; when the step size is big and the system responds quickly, the solar system may not function at its true maximum PowerPoint, and the fluctuation around the maximum power point will cause. The smaller the threshold, the closer the ultimate functioning point is to the maximum power point in principle, but in practice, if the threshold is set too low, the system will not attain a steady-state and will eventually fluctuate within a given range.

Fuzzy Logic Controllers are excellent at modeling nonlinear systems. It performs the needed procedures using linguistic variables. It's a simple and practical approach to establishing a nonlinear system's properties throughout implementation and design. Fuzzification, fuzzy inference, and defuzzification are the three primary components of the Fuzzy Logic Controller.

## III. Fuzzy Logic Based Buck-Boost Converter

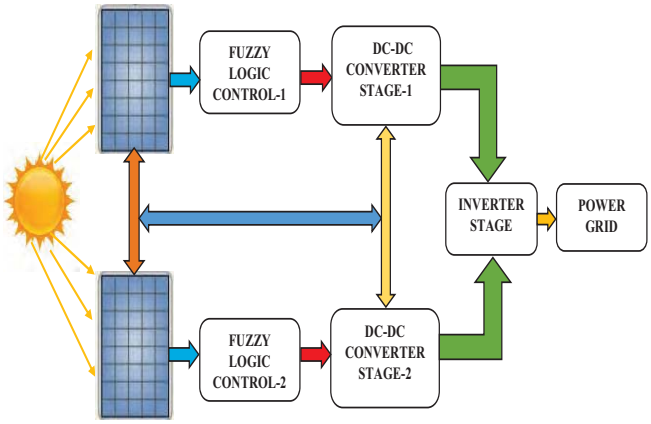


Figure 1. Block diagram of proposed FLBBC

The block diagram and circuit diagram of the proposed FLBBC are illustrated in fig.1 & fig.2. FLBBC is made up of two stages: a dc-dc converter stage and an inverter stage. The dc-to-dc converter stage contains two dc to dc converter sections $CHOP_1$ and $CHOP_2$ deals with the two sub-arrays $PV_1$ and $PV_2$ of the solar PV array. Fuzzy logic control-1 is employed to give gating pulses for the switches of dc-dc converter-1 and fuzzy logic control-2 is employed to give gating pulses for the switches of dc-dc converter-2.

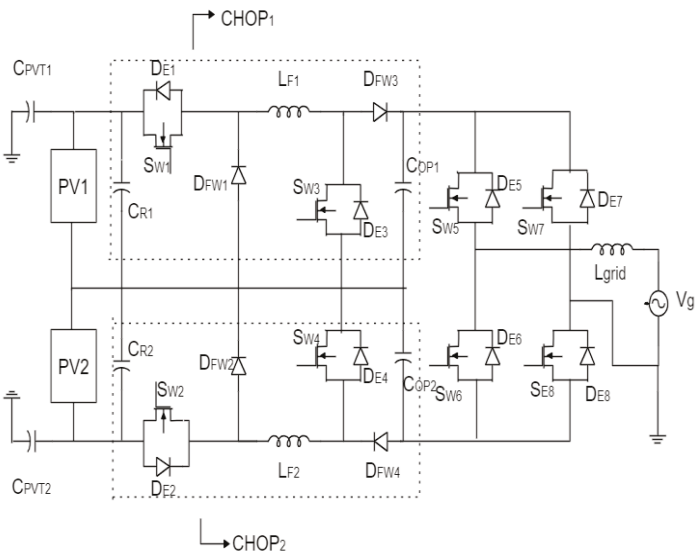


Figure 2. Circuit diagram of proposed FLBBC

The dc to dc converter section $CHOP_1$ is consisting of the switching device, $S_{W1}$ along with its anti-parallel diode, $D_{E1}$, $S_{W3}$ along with its anti-parallel diode, $D_{E3}$, the freewheeling diodes, $D_{FW1}$, $D_{FW3}$ and the filter inductor $L_{F1}$, and capacitors, $C_{R1}$, and $C_{OP1}$. Similarly, the dc to dc converter section $CHOP_2$ is consisting of the switching device, $S_{W2}$ along

E-ISSN 2581 – 7957
P-ISSN 2277 – 3916
CVR Journal of Science and Technology, Volume 22, June 2022
DOI: 10.32377/cvrjst2210

with its anti-parallel body diode, $D_{E2}$, $S_{W4}$ along with its anti-parallel body diode, $D_{E4}$, the freewheeling diodes, $D_{FW2}$, $D_{FW4}$ and the filter inductor $L_{F2}$, and capacitors, $C_{R2}$, and $C_{OP2}$. The inverter section is consisting of the switching devices, $S_{W5}$, $S_{W6}$, $S_{W7}$, $S_{W8}$, and their corresponding diodes, $D_{E5}$, $D_{E6}$, $D_{E7}$ and $D_{E8}$ respectively. The inverter section is combined with the grid through the filter inductor, $L_{grid}$. The stray capacitance of the PV array to the ground is modeled by the two capacitors, $C_{PVT1}$ and $C_{PVT2}$.

$CHOP_1$ operates in buck mode when $V_{PV1} \geq V_{COP1}$, while $CHOP_2$ operates in buck mode when $V_{PV2} \geq V_{COP2}$. Here $V_{PV1}$, $V_{PV2}$ are the MPP voltages of $PV_1$ & $PV_2$ and $V_{COP1}$, $V_{COP2}$ are the output voltages of $CHOP_1$ and $CHOP_2$ respectively. During buck mode duty ratios of the switches, $S_{W1}$ and $S_{W1}$ are varied sinusoidally to ensure sinusoidal grid current ($I_g$) while $S_{W3}$ and $S_{W4}$ are kept off. $CHOP_1$ operates in boost mode when $V_{PV1} \leq V_{COP1}$, while $CHOP_2$ operates in boost mode when $V_{PV2} \leq V_{COP2}$. During boost mode duty ratios of the switches, $S_{W3}$ and $S_{W4}$ are varied sinusoidally to ensure sinusoidal $I_{grid}$ while $S_{W1}$ and $S_{W1}$ are kept on throughout this mode. The sinusoidal switching pulses of the switches $CHOP_1$ and $CHOP_2$ are synchronized with the grid voltage ($V_{grid}$), to accomplish unity power factor operation. The switches, $S_{W5}$ and $S_{W8}$ are kept on and switches $S_{W6}$ and $S_{W7}$ are kept off permanently during the entire positive half cycle. While during the entire negative half cycle, the switches, $S_{W6}$ and $S_{W7}$ are kept on and switches, $S_{W5}$ and $S_{W8}$ are kept off permanently.

## IV. FLBBC Control Strategy

### A. Control Strategy

Gate triggering pulses for the switching devices are generated to operate both the subarrays at their respective MPP and to ensure the flow of sinusoidal grid current in phase with the grid voltage. Two MPP tracking algorithms are used to generate two separate reference voltages $V_{mppt1}$ and $V_{mppt2}$ for the two subarrays. These reference voltages $V_{mppt1}$ and $V_{mppt2}$ are compared with the sensed subarray voltages $V_{pv1}$ and $V_{pv2}$ and the errors generated are processed through two separate fuzzy logic controllers. The detailed flow diagram is shown in fig.3. The reference current of inductor $L_1$ is $I_{L1ref}$ and inductor $L_2$ is $I_{L2ref}$. The sensed inductor currents $I_{L1}$ and $I_{L2}$ are compared with their corresponding references $I_{L1ref}$ and $I_{L2ref}$. The errors obtained are processed through the two separate fuzzy logic controllers to generate the required sinusoidal duty ratios for the switches $S_1$ and S2 during buck mode. Similarly, the two separate fuzzy logic controllers are engaged to process the generated errors and generate the required sinusoidal duty ratios for switches $S_3$ and $S_4$ during boost mode. Pulse width modulation (PWM) generator is used to generate gating signals for the switches of inverter $S_5$, $S_6$, $S_7$, $S_8$.

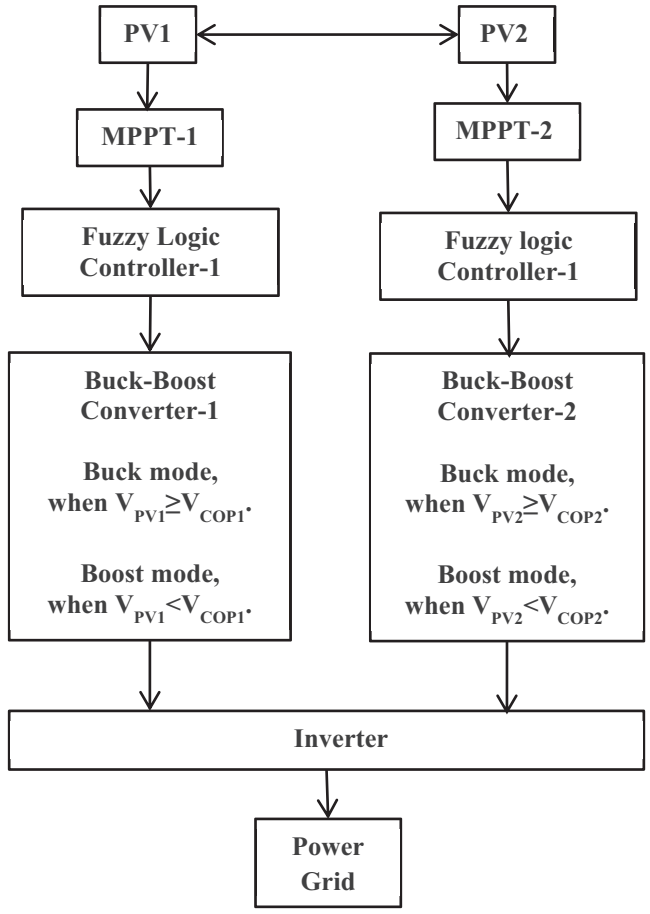


Figure 3. Control flow of the fuzzy logic-based buck-boost converter

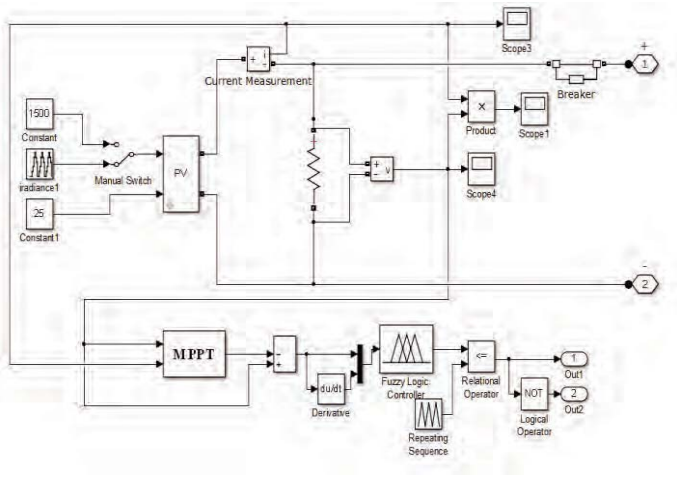


Figure 4. Control configuration of the buck-boost inverter

Using the photovoltaic effect, a photovoltaic cell turns sunlight into an electric current. When PV cells are linked in

CVR Journal of Science and Technology, Volume 22, June 2022
DOI: 10.32377/cvrjst2210

series, the voltage is increased. When PV cells are linked in series, the current is increased. Two PV arrays are connected in series and each PV array is employed with a separate MPPT and fuzzy logic controller. The proposed FLBBC operates in buck mode when the sensed voltage of PV1 is greater than the capacitor voltage COP1 and the sensed voltage of PV2 is greater than the capacitor voltage COP2. FLBBC operates in boost mode when the sensed voltage of PV1 is less than the capacitor voltage COP1 and the sensed voltage of PV2 is less than the capacitor voltage COP2. To provide voltage or current feedback control, switching regulators employ a duty cycle. The duty cycle is the ratio of the turn-on time (TON) to the turn-off time (TOFF), and it provides a straightforward connection between the input and output voltages. The duty cycle of a switching regulator is determined by the topology of the switching regulator. The duty cycle of a step-down (buck) converter is D, where D = output voltage/input voltage. The duty cycle of a step-up (boost) converter is D = 1 – (input voltage/output voltage). The detailed control configuration is shown in Fig.4.

### *B. Fuzzy Controller Design*

Fuzzy control is a technique that permits nonlinear controllers to be built using heuristic information derived from expert knowledge. The input signals are processed by the fuzzification block, which assigns them a fuzzy value.

The set of rules is based on process knowledge and provides for a linguistic description of the variables to be managed. The inference mechanism oversees determining how the rules and their membership functions should be interpreted. The defuzzification block converts the fuzzy information from the inference mechanism into non-fuzzy information that can be used to manage the operation.

## V. Results & Discussion

To validate the effectiveness of the proposed FLBBC comprehensive simulation studies are performed on MATLAB and shown in fig.5. The simulation study's major goal is to examine the FLBBC performance while both PV subarrays are experiencing a large difference in irradiance. The several parameters that are used for the simulation studies are listed in Table I. The MPP parameters of each sub-array at standard test state (STS) are as follows: Vpv1 = Vpv2 = 116 V, Ipv1= Ipv2 = 5.7A and Ppv1 =Ppv2 = 661W. The fluctuation in irradiance level concerning time for the two sub-arrays that are used to illustrate the efficacy of the proposed inverter is tabulated in Table II. The variation in the insolation level of $PV_1$ is indicated in Table II while the insolation level of $PV_2$ is maintained at 0.8 kW/m$^2$.

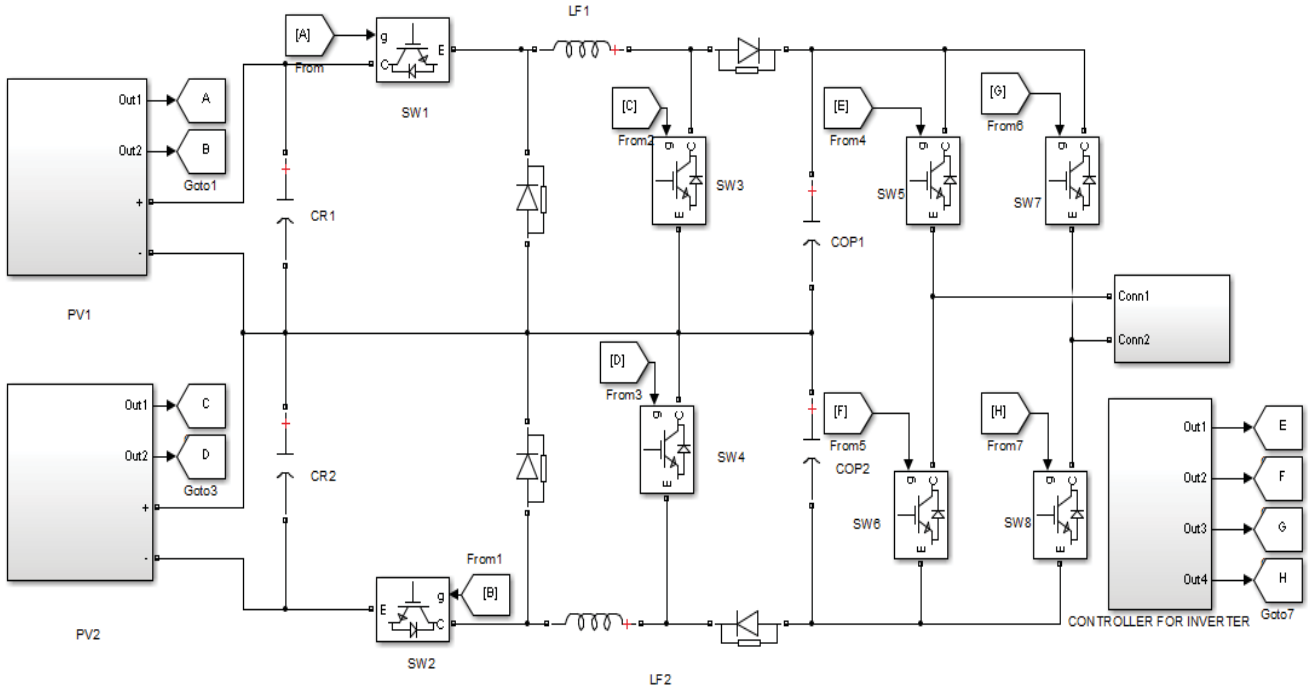


Figure 5. Simulation diagram of proposed buck-boost inverter

TABLE I.
APPLIED VARIATIONS ON INSOLATION AND TEMPERATURE OF TWO SUB ARRAYS

| Time in second | 0-1 | 01-2 | 22-3 | 33-4 | 44-5 | 55-6 | 66-7 | 77-8 |
|---|---|---|---|---|---|---|---|---|
| Irradiance on $PV_1$ (kW/$m^2$) | 0.5 | 0.6 | 0.7 | 0.8 | 0.9 | 1.0 | 1.0 | 1.0 |
| Irradiance on $PV_2$ (kW/$m^2$) | 0.8 | 0.8 | 0.8 | 0.8 | 0.8 | 0.8 | 0.8 | 0.8 |
| Temperature in $PV_1$ ($^\circ C$) | 25 | 225 | 225 | 225 | 225 | 225 | 225 | 325 |
| Temperature in $PV_2$ ($^\circ C$) | 225 | 225 | 225 | 225 | 225 | 225 | 225 | 225 |

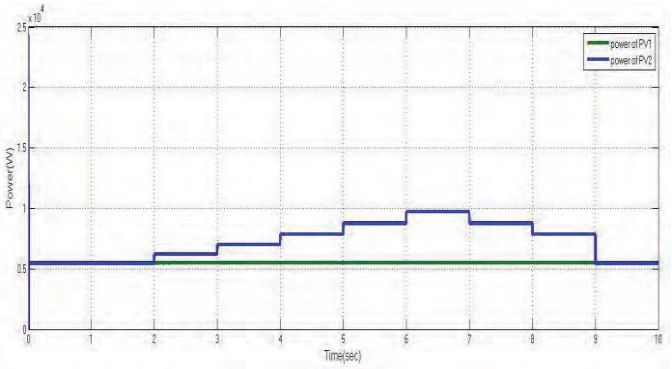


Figure 6. Variation in $P_{pv1}$ and $P_{pv2}$ during the entire range of operation

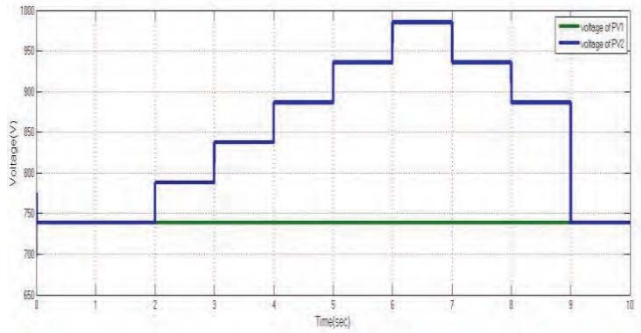


Figure 7. Variation in $V_{pv1}$ and $V_{pv2}$ during the entire range of operation

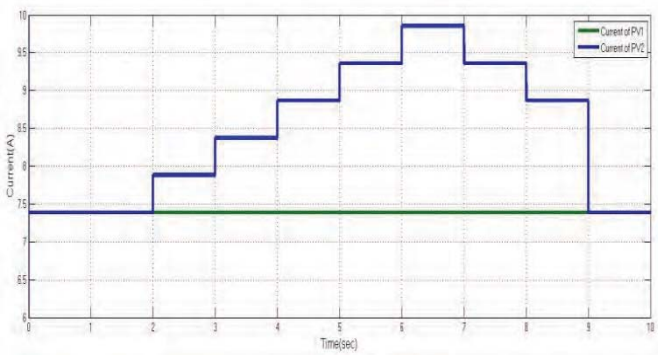


Figure 8. Variation in $I_{pv1}$ and $I_{pv2}$ during the entire range of operation

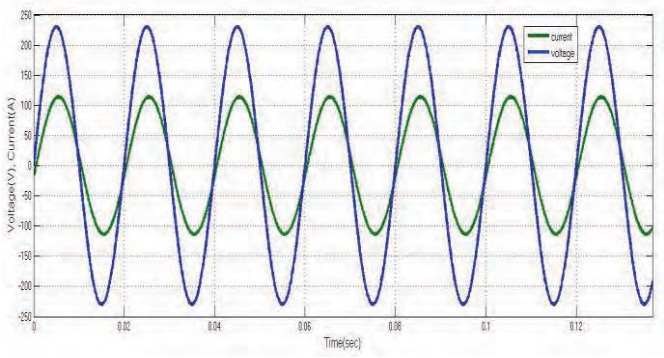


Figure 9. Grid current in phase with the grid voltage

The pulse width modulation generator is used to generate gate triggering pulses for these switches. A single-phase voltage source is used as the power grid connected to the output terminals of the inverter. A filter inductor is connected between the inverter and the power grid. Each PV array is connected to the ground by using stray capacitance.

Figures 6–9 show the change in $P_{pv1}$, $P_{pv2}$, $V_{pv1}$, $V_{pv2}$, $I_{pv1}$, $I_{pv2}$ throughout the range of variation in the irradiance levels indicated in Table II. These waveforms indicate that the proposed inverter can extract maximum power from two sub-arrays operating under MOC. Two different magnitudes of power are drawn from the two sub-arrays. When different magnitudes of power are supplied to the grid it is needed to maintain the grid current is sinusoidal and in phase with the grid voltage. This can be achieved by providing the proper gate triggering pulses for the switching devices of the proposed FLBBC. The reference voltages are compared with the sensed voltages across the capacitors $C_{OP1}$ and $C_{OP2}$. If the sensed voltage is greater than the reference voltage the FLBBC operates in buck mode and sensed voltage is less than the reference voltage the FLBBC operates in boost mode. The voltage across the output capacitors is maintained constant. From Fig.10. It can be concluded that when two different magnitudes of power are supplied to the grid the grid current is sinusoidal and in phase with the grid voltage. This can be achieved by using the proposed FLBBC.

The simulation diagram of the proposed FLBBC is connected as per the circuit diagram and shown in fig.6. The PV array is designed using the equivalent circuit of a photovoltaic cell. The irradiance of the PV1 is varied concerning time and the irradiance of the PV2 is kept constant at 0.8kW/m2. The temperatures on both PV panels are kept constant at 25◦C. The insulated gate bipolar transistor (IGBT) is used as a switching device because of its high voltage capability. Each self-commutated switch is connected to its anti-parallel diode. A freewheeling diode connected between the two self-commutated switches in both buck-boost converters. A filter inductor is also connected between the self-commutated switches. Two output capacitors are connected between the dc-dc converter stage and the inverter stage to provide a constant input voltage to the inverter. The inverter section consists of four self-commutated switches.

TABLE II.
COMPARISON OF VARIOUS TRANSFORMERLESS SCHEMES

| Schemes | $N_{PVA}$ | $N_{PVO}$ | $V_{IN}$ | $E_{MOC}$ |
|---|---|---|---|---|
| **H-bridge based [1]** | 1 | 1 | $>V_m$ | High |
| **NNC based [2]** | 1 | 1 | $>2V_m$ | Highest |
| **TSGI based [12]** | 2 | 2 | $<V_m$ | Low |
| **BBBBI based [18]** | 1 | 1 | $<V_m$ | Low |
| **Proposed FLBBC** | 2 | 2 | $<V_m$ | Lowest |

A comparison of several aspects of the proposed scheme with previous transformerless methods such as the H-Bridge-based scheme, the NNC-based scheme, transformerless single-phase grid-connected inverter (TSGI) scheme, and boost in boost, buck in buck inverter (BBBBI) scheme are tabulated in Table III. $N_{PVA}$ is referred to as the required number of PV arrays/subarrays, $N_{PVO}$ is referred to as the number of PV arrays operated together, $V_{IP}$ is referred to as the input voltage requirement, $E_{MOC}$ is referred to as the chance of being impacted by MOC. The fuzzy logic controller gives the required gate triggering pulses to the switches of the buck-boost converter depending on the MOC. Based on the objective comparison in Table III, the proposed FLBBC is the most successful method in dealing with MOC.

Advantages of FLBBC over previous transformerless schemes

- Maximum power extraction from two different PV panels, regardless of their environmental conditions.
- Because it is a buck-boost inverter, it can handle a broad range of PV panel voltages.
- The inverter's neutral point clamped-based construction eliminates the problem of leakage current.
- There is no shoot-through fault in the inverter.
- For the operation FLBBC, it is not necessary to sense grid current.

## VI. CONCLUSIONS

In this paper, a fuzzy logic-based buck-boost converter is proposed to deal with the mismatched operating conditions on the PV arrays. The number of serially linked PV modules is less, so the effect of shading on the PV modules is minimized. The proposed FLBBC ensure that the two serially linked PV arrays are controlled together and operate at their respective MPPT. As a result, it was well suited for PV subarrays with mismatched operating conditions. The suggested inverter's topological structure and control technique ensure that the amount of leakage current associated with PV arrays stays within the permitted limit. Power from both PV arrays is delivered to the grid simultaneously while maintaining the grid current is sinusoidal and in phase with the grid voltage. This is achieved by employing separate FLBBC for both PV arrays. A fuzzy logic controller is used to generate the required gate triggering pulses for the switches of the buck-boost converter. By using the proposed FLBBC, the operating efficiency of the system is increased. The effectiveness of the proposed FLBBC is validated by comprehensive simulation studies. By using the proposed FLBBC, two serially connected PV arrays are controlled simultaneously at their respective MPPT. Furthermore, this FLBBC is designed to operate several PV arrays controlled together at their respective MPPT. The environmental mismatch conditions are high in solar farms because of their large space. Due to this, the power output from solar farms is greatly reduced. Furthermore, FLBBC can be employed in solar farms to maximize power yield and increase efficiency.

## REFERENCES

[1] Araújo, Samuel Vasconcelos, Peter Zacharias, and Regine Mallwitz. "Highly efficient single-phase transformer less inverters for grid-connected photovoltaic systems." *IEEE Transactions on Industrial Electronics* 57.9 (2009): 3118-3128.

[2] Xiao, Huafeng, and Shaojun Xie. "Transformer less split-inductor neutral point clamped three-level PV grid-connected inverter." *IEEE transactions on power electronics* 27.4 (2011): 1799-1808.

[3] Bidram, Ali, Ali Davoudi, and Robert S. Balog. "Control and circuit techniques to mitigate partial shading effects in photovoltaic arrays." *IEEE Journal of Photovoltaics* 2.4 (2012): 532- 546.

[4] Kaushika, Narendra D., and Nalin K. Gautam. "Energy yield simulations of interconnected solar PV arrays." *IEEE Transactions on Energy Conversion* 18.1 (2003): 127-134.

[5] Patel, Hiren, and Vivek Agarwal. "Maximum power point tracking scheme for PV systems operating under partially shaded conditions." *IEEE transactions on industrial electronics* 55.4 (2008): 1689-1698.

[6] Velasco-Quesada, Guillermo, et al. "Electrical PV array reconfiguration strategy for energy extraction improvement in grid-connected PV systems." *IEEE Transactions on Industrial Electronics* 56.11 (2009): 4319-4331.

[7] Villa LF, Ho TP, Crebier JC, Raison B. A power electronics equalizer application for partially shaded photovoltaic modules. IEEE Transactions on Industrial Electronics. 60.3 (2012):1179-90.

[8] Shimizu, Toshihisa, Osamu Hashimoto, and Gunji Kimura. "A novel high-performance utility-interactive photovoltaic inverter system." *IEEE transactions on power electronics* 18.2 (2003): 704-711.

[9] Sharma, Pooja, and Vivek Agarwal. "Maximum power extraction from a partially shaded PV array using shunt-series compensation." *IEEE journal of photovoltaics* 4.4 (2014): 1128- 1137.

[10] Olalla, Carlos, et al. "Performance of power-limited differential power processing architectures in mismatched PV systems." *IEEE Transactions on Power Electronics* 30.2 (2014): 618-631.

[11] Elserougi AA, Diab MS, Massoud AM, Abdel-Khalik AS, Ahmed S. A switched PV approach for extracted maximum power enhancement of PV arrays during partial shading. *IEEE Transactions on Sustainable Energy*. 6.3 (2015):767-72.

[12] Debnath D, Chatterjee K. Maximising power yield in a transformerless single-phase grid connected inverter servicing two separate photovoltaic panels. *IET Renewable Power Generation*. 10.8 (2016):1087-95.

[13] Abbaszadeh, M. A., Monfared, M., & Heydari-doostabad, H., "High Buck in Buck and High Boost in Boost Dual-Mode Inverter,". *IEEE Transactions on Industrial Electronics*, 68.6 (2020): 4838-4847.

[14] R.Vijay and J. Durga Devi. “Optimal placement and sizing of wind-PV integrated power generation by ant colony optimization technique,” International Journal of Recent Trends in Engineering & Research 3.5(2017): 2455-1457.
[15] Raviprabakaran, Vijay, and Ravichandran Coimbatore Subramanian. "Enhanced ant colony optimization to solve the optimal power flow with ecological emission." International Journal of System Assurance Engineering and Management 9.1 (2018): 58-65.
[16] Vijay, Raviprabakaran. "Quorum sensing driven bacterial swarm optimization to solve practical dynamic power ecological emission economic dispatch." International Journal of Computational Methods 15.03 (2018): 1850089.
[17] Sedaghati, F., & Pourjafar, S. Analysis and implementation of a boost DC–DC converter with high voltage gain and continuous input current. *IET Power Electronics*, 13.4 (2020):798-807.
[18] Wu W, Ji J, Blaabjerg F. Aalborg inverter-a new type of “buck in buck, boost in boost” grid-tied inverter. IEEE Transactions on power electronics. 30.9 (2014):4784-93.